

This is an Open Access document downloaded from ORCA, Cardiff University's institutional repository: <https://orca.cardiff.ac.uk/id/eprint/103391/>

This is the author's version of a work that was submitted to / accepted for publication.

Citation for final published version:

Stamoulis, Catherine, Vanderwert, Ross , Zeanah, Charles H., Fox, Nathan A. and Nelson, Charles A. 2017. Neuronal networks in the developing brain are adversely modulated by early psychosocial neglect. *Journal of Neurophysiology* , jn.00014.2017. 10.1152/jn.00014.2017

Publishers page: <http://dx.doi.org/10.1152/jn.00014.2017>

Please note:

Changes made as a result of publishing processes such as copy-editing, formatting and page numbers may not be reflected in this version. For the definitive version of this publication, please refer to the published source. You are advised to consult the publisher's version if you wish to cite this paper.

This version is being made available in accordance with publisher policies. See <http://orca.cf.ac.uk/policies.html> for usage policies. Copyright and moral rights for publications made available in ORCA are retained by the copyright holders.



1 **Neuronal networks in the developing brain are adversely modulated by early psychosocial neglect**

2  
3 Catherine Stamoulis<sup>1,2,3\*</sup>, Ross E. Vanderwert<sup>8</sup>, Charles H. Zeanah<sup>5</sup>, Nathan A. Fox<sup>6</sup>, Charles, A. Nelson<sup>1,4,7</sup>

4  
5 <sup>1</sup>Harvard Medical School, Boston MA, USA

6 <sup>2</sup>Division of Adolescent Medicine, Boston Children's Hospital, Boston MA, USA

7 <sup>3</sup>Department of Neurology, Boston Children's Hospital, Boston, MA, USA

8 <sup>4</sup>Division of Developmental Medicine, Boston Children's Hospital, Boston MA USA

9 <sup>5</sup>Department of Psychiatry and Behavioral Sciences, Tulane University, New Orleans, LA, USA

10 <sup>6</sup>Department of Human Development and Quantitative Methodology, University of Maryland, College Park,  
11 MD, USA

12 <sup>7</sup>Graduate School of Education, Harvard University, Cambridge MA, USA

13 <sup>8</sup>School of Psychology, Cardiff University, UK

14  
15 \*To whom correspondence should be addressed: [caterina.stamoulis@childrens.harvard.edu](mailto:caterina.stamoulis@childrens.harvard.edu)

16  
17 Corresponding author address: Boston Children's Hospital, Division of Adolescent Medicine, 300 Longwood  
18 Avenue, Boston MA 02115

19  
20 Running title: Effects of early psychosocial neglect on brain networks

25 **Abstract**

26

27 The brain's neural circuitry plays a ubiquitous role across domains in cognitive processing and undergoes  
28 extensive re-organization during the course of development in part as a result of experience. In this paper we  
29 investigated the effects of profound early psychosocial neglect associated with institutional rearing on the  
30 development of task-independent brain networks, estimated from longitudinally acquired  
31 electroencephalographic (EEG) data from <30 to 96 months, in three cohorts of children from the Bucharest  
32 Early Intervention Project (BEIP), including abandoned children reared in institutions who were randomly  
33 assigned either to a foster care intervention or to remain in care as usual and never institutionalized children.

34

35 Two aberrantly connected brain networks were identified in children that had been reared in institutions: 1) a  
36 hyper-connected parieto-occipital network, which included cortical hubs and connections that may partially  
37 overlap with default-mode network and 2) a hypo-connected network between left temporal and distributed  
38 bilateral regions, both of which were aberrantly connected across neural oscillations. This study provides the  
39 first evidence of the adverse effects of early psychosocial neglect on the wiring of the developing brain. Given  
40 these networks' potentially significant role in various cognitive processes, including memory, learning, social  
41 communication and language, these findings suggest that institutionalization in early life may profoundly  
42 impact the neural correlates underlying multiple cognitive domains, in ways that may not be fully reversible in  
43 the short term.

44

45

46

47

48

49 **New and noteworthy**

50 This paper provides first evidence that early psychosocial neglect associated with institutional rearing  
51 profoundly affects the development of the brain's neural circuitry. Using longitudinally-acquired  
52 electrophysiological data from the Bucharest Early Intervention Project (BEIP), the paper identifies multiple  
53 task-independent networks that are abnormally connected (hyper- or hypo-connected) in children reared in  
54 institutions compared to never-institutionalized children. These networks involve spatially distributed brain  
55 areas and their abnormal connections may adversely impact neural information processing across cognitive  
56 domains.

57

58

59 **Keywords:** Brain networks, EEG, early development, psychosocial neglect

## 60 **Introduction**

61 From the microscale of individual neurons to the macroscale of cortical regions, the brain's neuroarchitecture  
62 is characterized by networks organized into topologies that ensure flexible, rapid and efficient neural  
63 information processing (Bullmore & Sporns, 2009). These networks may be divided into two broad categories:  
64 task-related networks that are activated and coordinated in response to cognitive demands and external stimuli,  
65 and task-independent (resting-state or stimulus-independent) networks that are spontaneously active and  
66 coordinated when the brain is not actively engaged in specific cognitive tasks. In some cases, task-dependent  
67 networks increase their activity and coordination at the same time as specific task-independent networks  
68 decrease theirs (Fox et al., 2005). Thus, in part due to these inverse correlations, task-independent networks  
69 may play a critical role in cognitive function and neural information processing (Raichle et al., 2001, 2007;  
70 Dosenbach et al., 2008; Kelly et al., 2008). Predominantly fMRI studies in adults have identified several  
71 distinct, and in some cases inter-connected task-independent networks, including the default-mode network  
72 (DMN) (Greicius et al., 2003; Vincent et al., 2006; Mantini et al., 2007; Ward et al., 2014). The topologies of  
73 these networks, estimated from fMRI data with excellent spatial resolution, may be directly correlated with  
74 those of structural networks (Greicius et al., 2009; Barttfelt et al., 2015). Previous studies have associated  
75 disrupted task-independent networks, with neuropsychiatric disorders, including schizophrenia and autism  
76 (Kennedy et al., 2006, Bluhm et al., 2007).

77  
78 The dynamic evolution of task-independent networks in the developing brain is poorly understood and our  
79 current knowledge is primarily based on fMRI studies. Elements of these networks come on line early in  
80 infancy (Fransson et al., 2007), but at least the DMN, which includes the ventral medial prefrontal cortex,  
81 anterior cingulate cortex (ACC), posterior cingulate cortex (PCC), lateral temporal cortex, precuneus and  
82 lateral parietal inferior gyri and the hippocampal formation (Greicius et al., 2003; Buckner et al., 2008), may  
83 be incompletely connected even at ages 7-9 years (Fair et al., 2008). Negative early experiences and stressors,

84 including poverty, abuse and psychosocial neglect, may have profound effects on neural maturation and  
85 consequently brain structure and function. In fact, social and emotional deprivation associated with  
86 institutional rearing has been shown to adversely affect brain's structure (Eluvathingal et al., 2006; Bauer et  
87 al., 2009; Sheridan et al, 2012; Bick et al., 2015), metabolism (Chugani et al., 2001; Tottenham et al., 2011)  
88 and electrical activity (Marshall et al., 2004, 2008; Vanderwert et al., 2010; McLaughlin et al., 2010, 2011;  
89 Stamoulis et al, 2015). Earlier work on the Bucharest Early Intervention Project (BEIP), a longitudinal study  
90 of children with a history of severe early deprivation (see Zeanah et al., 2003; Nelson et al., 2014), has shown  
91 that early psychosocial deprivation significantly impacts age-related dynamics in the developing brain's  
92 rhythms (Stamoulis et al., 2015). In the same sample, Marshall et al. (2008) showed that removal from an  
93 institution and placement in a foster care home prior to 24 months of age resulted in higher local network  
94 synchrony and statistically higher power in the alpha band (8-12 Hz) in the first 4 years of life in comparison  
95 to children who remained in institutions. A positive modulatory effect of foster care placement was also  
96 reported in other oscillations (Stamoulis et al., 2015), although changes in these oscillations from 42 to 96  
97 months were found to be distinct in children removed from institutions and placed in foster care compared to  
98 those who had never been institutionalized. These results highlight the profound adverse effects of early  
99 institutionalization on the developing brain.

100  
101 There are very few studies that have investigated task-independent networks in the developing brain and no  
102 previous work on the effects of neglect on these networks. This study investigated the topologies of task-  
103 independent networks and their developmental trajectories in children participating in the BEIP. Longitudinal  
104 electrophysiological (EEG) data from 3 cohorts were analyzed, including a group of institutionalized children  
105 who were randomized to a high-quality foster care placement (the foster care group), a group randomized to  
106 remain in institutional care (care as usual group) and a group of children who had never been institutionalized  
107 and lived with their families in the Bucharest community (never institutionalized group). Although EEG has

108 excellent temporal resolution, it lacks the high spatial resolution of fMRI and cannot resolve network  
109 topologies with the same spatial specificity as fMRI. Consequently, brain network topologies estimated from  
110 fMRI (which measures hemodynamic responses) and EEG (which measures neural activity) are not directly  
111 comparable. Nevertheless, EEG may still provide spatially sparse connectivity information on task-  
112 independent networks that may overlap with those identified by fMRI. Here we hypothesized that the spatial  
113 organization, properties and age-related dynamics of these networks are significantly impacted by early  
114 neglect in a frequency-specific manner, resulting in aberrant topologies that impair the efficiency of neural  
115 information processing and consequently cognitive function.

116

## 117 **Materials and Methods**

### 118 **1. Bucharest Early Intervention Project (BEIP)**

119 The BEIP is an ongoing longitudinal study that started in 2001 as a randomized controlled trial with foster care  
120 as an intervention for young children who had been abandoned at birth and placed in institutions. Using multi-  
121 modal data, the study aims to investigate the effects of early psychosocial deprivation on the structure and  
122 function of the developing brain and potentially beneficial effects of removal from an institution and foster  
123 care placement (Zeanah et al, 2003, Nelson et al, 2014). One hundred thirty-six children who had been reared  
124 in institutions entered the trial at ages 6-30 months, and were randomized to two arms, care as usual (CAUG;  
125  $n = 68$ ), i.e., more prolonged institutional rearing and foster care (FCG;  $n = 68$ ), i.e., placement in high-quality  
126 foster care specifically created for the project. A comparison group of 72 Romanian children who had never  
127 been institutionalized and lived with their families in Bucharest communities were also recruited (NIG).

128

### 129 **2. Participants**

130 The present study sought to quantify the age-related changes in task-independent networks using  
131 longitudinally acquired EEG signals from the BEIP cohorts, with an emphasis on 42 and 96 months (although

132 data at all ages were analyzed). Thus, only subgroups of the BEIP cohorts with measurements at a minimum of  
133 2 time points were included. Also, 4 children in the CAUG with diagnosed Autism Spectrum Disorder (ASD)  
134 were excluded. The characteristics of these groups are described in more detail in (Stamoulis et al., 2015).  
135 Sixty-two children in the CAUG (median age at study entry = 23.0 months, inter-quartile range (IQR) = 9  
136 months), 61 children in the FCG (median age at study entry = 23.0 months, IQR = 11 months), and 44 children  
137 in the NIG (median age at study entry = 21.5 months, IQR = 12 months) were studied.

138

### 139 **3. Demographic data**

140 Age, which varied between participants both at study entry and the second assessment (30-33 months) but not  
141 at 42 or 96 months, gender, age at foster care placement for children in the FCG, percent time spent in  
142 institutions for children in the FGC and CAUG, birth weight and head circumference were included in the  
143 analysis as potential covariates. All missing data were assumed to be missing at random, mainly as a result of  
144 longitudinal attrition. Eighty-four females and 83 males were studied. Birth weight varied in the range 0.9 –  
145 4.5 kg (median = 3.0 kg, IQR = 0.8 kg). These data were missing in 15 children. There were no statistically  
146 significant differences in birth weight between the CAUG and FCG (median of CAUG = 2.8 kg, median of  
147 FCG = 2.6 kg,  $p = 0.14$ ) but both groups had statistically lower birth weights than the NIG (median of NIG =  
148 3.3 kg,  $p < 0.001$ ). Head circumference was measured at all 4 time points. These data were missing for 17  
149 children at baseline, 16 at 30 months, 25 at 42 months and 32 at 96 months. Median circumference at baseline  
150 was 46.8 cm, IQR = 2.5 cm, 48.0 cm at 30 months IQR = 2.0 cm, 48.6 cm at 42 months, IQR = 1.6 cm, and  
151 51.0 cm at 96 months, IQR = 2 cm. There were no significant differences in head circumference between the  
152 CAUG and FCG at any age ( $p = 0.18$  at baseline,  $p = 0.07$  at 30 months,  $p = 0.09$  at 42 months,  $p = 0.38$  at 96  
153 months). In the FCG, age at foster care placement was in the range 6.8 – 33 months, median = 24.8 months,  
154 IQR = 10.1 months. Time spent at institutions at baseline, 42 and 96 months is summarized in Table S1.

155



#### 156 **4. EEG data characteristics and pre-processing**

157 EEGs were collected at study entry (baseline) as well as at 30-33, 42 and 96 months, using an Electro-Cap  
158 (Electro-Cap International Inc) system (12 scalp electrodes: F3, F4, Fz, C3, C4, P3, P4, Pz, T7, T8, O1, O2).  
159 The characteristics of these data are described in detail in (Marshall et al, 2008, Vanderwert et al, 2010,  
160 Stamoulis et al, 2015). At baseline, 30-33 months and 42 month assessments, task-independent EEG signals  
161 were recorded while lights were turned off for ~1-3 min. At 96 months, task-independent EEG signals were  
162 recorded during 1-min intervals of eyes-closed (EC) and eyes-open (EO). Only signals recorded under the EC  
163 condition were included in the analysis. Data were sampled at 512 samples/s and bandpass filtered during  
164 acquisition in the range 0.1- 100 Hz. Prior to analysis all signals were referenced to an average reference.  
165 Previous work has shown that in the absence of appropriate source modeling, which is difficult with a small  
166 number of electrodes, an average reference results in substantially lower connectivity errors than a mastoid or  
167 Cz reference (Chella et al, 2016). However, similar to all referencing approaches, an average reference has  
168 shortcomings, too, particularly for localizing specific EEG waveforms such as event-related potentials (ERP).  
169 Here, the issue of localization is of less concern. Also, several studies have shown that for connectivity  
170 analyses, even with a low number of EEG electrodes average referencing is preferable to the use of a common  
171 reference (Dien, 1998). A stopband filterbank of 3<sup>rd</sup> order elliptical filters with a 1-Hz bandwidth, 0.5 dB  
172 ripple in the passband and 20 dB in the stopband was used to suppress the power line noise at 50 Hz and its  
173 100-Hz harmonic. Artifacts associated with eye blinking were locally suppressed using a matched-filtering  
174 approach, where signal templates for eye blinks were used to detect intervals containing these artifacts  
175 (Stamoulis et al., 2009). Individual EEG signals were further denoised via signal decomposition and  
176 elimination of random components identified based on their autocorrelation function (Stamoulis et al., 2014).  
177 Finally, signals containing extreme amplitude outliers, i.e., above a threshold equal to the median plus 3 times  
178 the inter-quartile difference (Tukey, 1977) were also eliminated. These outliers are likely to be associated with  
179 broadband muscle and/or other non-neural activity. Consequently, 1-s intervals containing outliers were

180 excluded from the signal decomposition and mutual information estimations.

181

## 182 **5. Signal analysis**

183 **5a. Estimation of narrowband EEG signal components (individual oscillations):** Neural oscillations in the  
184 developing brain may have characteristic frequencies that do not fall within the limits of traditional biological  
185 bands (delta to ripple), established based on adult brain signals. Thus, frequency domain analysis of bandpass  
186 filtered signals in these bands may not be appropriate. Instead, a fully unsupervised, time-domain approach  
187 based on the Ensemble Empirical Mode Decomposition method (EEMD, Wu et al, 2005) was used to estimate  
188 neural oscillations and their dominant frequencies. The EEMD is a modification of the classical EMD method  
189 (Huang et al, 1998) and accounts of the problem of mode (component) mixing. The estimation process has  
190 been described in detail in previous work (Stamoulis et al., 2015). Task-independent network connectivity was  
191 estimated for individual oscillations of the EEG to construct frequency-specific networks. Briefly, each EEG  
192 signal was decomposed into a small set of narrowband components that significantly contributed to the  
193 broadband signal amplitude. The cost function proposed in (Stamoulis et al, 2011) was also used to select non-  
194 random components and eliminate noise-related signal contributions with substantial amplitude. A sliding 1-s  
195 window was used in all estimations. In exploratory analyses of the data, the window length was varied  
196 between 1 and 4 s, yielding similar estimates in oscillation amplitude, frequency and connectivity.

197

198 **Glossary of terms:** The following network parameters were estimated for each identified oscillation in the  
199 EEG: a) *spatially averaged connectivity* (over the entire brain and over individual networks identified in  
200 models to be statistically distinct between groups), b) non-directional *edge-specific connectivity* for each edge  
201 connecting pair of network nodes and c) *node centrality*, a measure of the importance of each node in the  
202 network. Each electrode was treated as a network node. Spatially-averaged and edge-specific connectivities  
203 were quantified using *mutual information*, an information theoretic measure (see 5b). Two types of

204 connectivity matrices were estimated for each child at each time point and each oscillation, a weighted  
205 connectivity matrix containing the actual mutual information values and thus the actual connection strengths  
206 between pairs of nodes and the adjacency matrix, a binary matrix of edge connection/non-connection obtained  
207 by appropriately thresholding the weighted connectivity matrix. Based on connectivity thresholds two sets of  
208 networks were identified, hyper- and hypo-connected networks (see 5c and 5d). Node centrality was quantified  
209 using node strength, a measure of the sum of its connections based the adjacency matrix (see 5e).

210

211 **5b. Estimation of oscillation-specific connectivity:** In the case of a large number of electrodes, connectivity  
212 analysis may be best conducted at the source level, to appropriately address issues of volume conduction  
213 which may impact various connectivity measures. The adequacy and accuracy of source connectivity analysis  
214 in the case of 12 electrodes are questionable, independently of the source separation or localization methods  
215 used. Information-based connectivity measures have been shown to be relatively robust to volume conduction  
216 (Vicente et al, 2011) and were used in this electrode-level analysis. Mutual information was used to quantify  
217 undirected pairwise network connectivity. Together with other information theoretic measures, it has been  
218 previously used in a number of studies to quantify correlation between electrophysiological signals and may  
219 be more robust to the inherent noise of these signals than other measures such as coherence (Vejmelka et al,  
220 2008; Schreiber, 2000; Palus et al, 2001; Stamoulis et al, 2013). Mutual information  $I(X, Y) = \sum_{x,y} p(x,$

221  $y) \log \frac{p(x, y)}{p(x)p(y)} \geq 0$ , between random variables  $X$  and  $Y$  measures their mutual dependence (Cover & Thomas,  
222 2004). It is a function of their joint and marginal probability density functions  $p(x, y)$ ,  $p(x)$  and  $p(y)$ , which  
223 were estimated using a kernel-based method (assuming a Gaussian kernel) following segmentation of EEG  
224 signals in 1-s windows. Across ages and participants, a kernel bandwidth of 0.8 was used in the estimation and  
225 the probability density functions were evaluated at 200 points.

226

227 **5c. Connectivity threshold estimation:** Edge-specific mutual information thresholds were estimated as

228 follows: for each oscillation and network edge, the median (across subjects) mutual information for the NIG  
 229 (and thus each age-matched oscillation and edges in the control group) was calculated as well as  
 230 corresponding 95% confidence intervals (CI), using bootstrapping with replacement (2000 draws and an  
 231 accelerated, bias-corrected percentile method (Efron, 1993)). The edge-specific upper CI for the NIG median  
 232 mutual information was selected as an edge's threshold for edge hyper-connectivity, and the corresponding  
 233 lower CI was selected as the threshold for edge hypo-connectivity.

234

235 **5d. Adjacency matrix estimation for relative hyper- and hypo-connectivity:** Based on the above  
 236 thresholds, two sets of adjacency matrices - with elements  $(i, j)$  for edges connecting nodes  $i$  and  $j$ , for each  
 237 oscillation-specific undirected graph were estimated for the CAUG and FCG, 1) the *hyper-connectivity*  
 238 *adjacency matrices*, with elements that were equal to 1 for edges that exceeded the upper CI for median  
 239 connectivity of the NIG and zeros elsewhere, 2) the *hypo-connectivity adjacency matrices*, with elements that  
 240 were equal to 1 for edges that were below the lower CI for median connectivity of the NIG and 0 elsewhere.

241

242 **5e. Estimation of node centrality:** The maximum number of possible connections of each node in the  
 243 estimated networks is 12 (a self-connection and 11 connections to all other nodes). There are several ways to  
 244 define *node centrality*, i.e., the importance of a node in a network. Here it is defined in two ways: 1) in terms  
 245 of *node strength*, i.e. the ratio of the sum of all edge weights for a node over the maximum possible sum of

246 weights, so for node  $c_i = \frac{\sum_j I_{ij}}{\max \sum_j I_{ij}}$ ; 2) in terms of *node connectedness*, i.e., the ratio of the sum of all

247 binary edge values for a node over the maximum possible sum of weights i.e.,  $c_i = \frac{\sum_j A_{ij}}{\max \sum_j A_{ij}}$ . Based on

248 these topological measures it is possible to identify potential *hubs*, i.e., highly connected nodes that are critical  
 249 for information processing through the network. Note that the adjacency matrices for the CAUG and FCG

250 were estimated as described in sub-section 5d. The adjacency matrices for subjects in the NIG were estimated  
251 assuming the median (across subjects and electrodes) MI as the corresponding connectivity threshold.

252

## 253 **6. Statistical analysis**

254 Differences in network characteristics at individual ages were assessed using ordinary linear regression  
255 models, with edge connectivity or node centrality as the dependent variable, and group (using criterion coding  
256 to avoid including several group variables given the relatively small sample), time spent in institutions, birth  
257 weight, head circumference, age at foster care placement and gender (categorized as female = 0, male = 1) as  
258 independent variables. In these models (as well as in mixed effects models used to assess age-related  
259 parameter changes), each edge or node parameter were assessed independently, i.e., nodes/edges were not  
260 compared to each other. Instead, their individual (independent) correlation with the predictors and confounders  
261 were assessed. Therefore, corrections for multiple comparisons were not necessary, particularly in mixed  
262 effects models (Gelman et al, 2012). Combinations of independent variables were included in separate models.  
263 Logistic regression models with group as the dependent variable (assuming the NIG as the reference category)  
264 and network measures as independent variables were also developed. Finally, in cases where network  
265 parameters were found to be statistically distinct among the 3 groups, their relationship was also investigated  
266 through logistic regression models that included only the CAUG (= 0) and FCG (= 1), i.e., the groups in the  
267 two arms of the randomized trial. All modeling approaches yielded consistent results. Note that at baseline  
268 (prior to the randomization) there were only two groups, institutionalized and never-institutionalized.

269

270 Linear mixed effects models were developed to investigate temporal trajectories of network characteristics.  
271 For all children randomized to the intervention arm, foster care placement occurred before 42 months of age.  
272 Therefore, to assess intervention-related effects we focused on changes in network parameters between 42 and  
273 96 months. Thus, the models included a subject-specific intercept and a subject-specific age slope, to account

274 for potential subject-specific variabilities. Independent variables included gender, birth weight, head  
275 circumference, group, age at foster care placement and percent time spent at institutions. Given the sample  
276 size, only relatively small models were developed with combinations of 1-3 independent variables. All  
277 analyses were done using the software Matlab (Mathworks, Inc, Natick MA, USA).

278

## 279 **Results**

280 We investigated oscillation-specific network properties at all 4 age assessments, and their developmental  
281 changes from 42 to 96 months. We first examined spatially-averaged (global) connectivity followed by edge-  
282 specific connectivity and node centrality. We conducted two complementary analyses: 1) Using connectivity  
283 thresholds derived from the NIG, we compared the FCG and the CAUG relative to NIG. We thus present  
284 results on abnormal networks in the FCG and CAUG that were found to be *hyper-connected* or *hypo-*  
285 *connected* relative to the NIG; 2) We compared all 3 groups to each other via statistical models that included  
286 adjustments for birth weight or head circumference. We report network measures only for subnetworks that  
287 were found to be statistically distinct in the 3 groups. As previously noted, regression models were also  
288 developed to compare only the CAUG and FCG, separately from the NIG. Statistically significant group  
289 differences in network parameters identified in these models were consistent with those identified using  
290 models that included the NIG.

291

### 292 **1. Brain-wide (spatially-averaged) connectivity**

293 First, median (over electrodes) mutual information (MI) that had been averaged in time was compared  
294 between groups for each estimated oscillation at each assessment age, to assess potential differences in  
295 brain/hemisphere-wide connectivity. Corresponding frequency-connectivity relationships at these ages  
296 (unadjusted for confounders or other covariates) are shown in Figure 1. Inter-quartile ranges (vertical bars for  
297 MI and horizontal bars for frequency) are shown. In these unadjusted connectivity data, no significant

298 differences were found between groups except for the gamma oscillation at 96 months ( $p = 0.012$ ), and the  
299 alpha and theta oscillations at baseline (study entry) ( $p = 0.002$  and  $p = 0.016$  for alpha and theta connectivity  
300 respectively). When adjusted for birth weight or head circumference, significant differences in whole brain  
301 and hemisphere-specific connectivity were estimated between institutionalized and never institutionalized  
302 children in the theta band at baseline ( $p = 0.006$  for the entire brain,  $p = 0.002$  for the left-hemisphere and  $p =$   
303  $0.034$  for the right hemisphere). When adjusted for age at foster care placement, significant group differences  
304 in left-hemisphere theta connectivity were estimated at 96 months ( $p = 0.035$ ). When adjusted for head  
305 circumference, significant group differences in beta connectivity were also estimated in the left hemisphere at  
306 96 months ( $p = 0.044$ ). The statistics of oscillation frequencies at each assessment age are summarized in  
307 Table S1.

308

## 309 **2. Network topologies at 4 assessment ages**

310 All reported connectivity parameters in the CAUG and FCG are relative to the corresponding NIG parameters.  
311 For each assessment age and oscillation, network topologies for the two groups are shown in Figure 2. Note  
312 that these connectivities are unadjusted for potential confounders and are solely based on thresholding of the  
313 MI matrices. Appropriate adjustments were included in the analysis and are described in the next section. For  
314 each oscillation, topologically distinct hyper- and hypo-connected subnetworks were identified in the CAUG  
315 and FCG with some overlap of their elements across oscillations. At baseline, both groups had a large number  
316 of hyper-connected edges (up to  $\sim 85\%$  of all possible edges) and a small number of hypo-connected edges.  
317 This number decreased significantly from baseline to the second assessment (from more than  $75\%$  to  $\sim 25\%$  of  
318 all possible connections), potentially due to neural maturation and elimination of redundant connections. No  
319 substantial topological differences were estimated between the two groups at those ages. At 42 months, an  
320 even lower number of hyper-connected edges were identified in both groups, asymmetrically clustered in the  
321 left hemisphere and primarily in temporo-parietal and parieto-occipital regions in the gamma and beta

322 networks, but less consistently (in space) in other networks. For some oscillations, a small number of hypo-  
323 connected edges were also identified. Finally, at 96 months, more consistent topologies were identified in both  
324 groups: a) a hyper-connected gamma network with aberrant connections between bilateral parietal and  
325 occipital regions; b) relatively larger hypo-connected beta and alpha networks with aberrant connections  
326 primarily between left and right temporal regions, left temporal and bilateral frontal and occipital regions.

327

### 328 **3. Network topologies and parameters at 42 and 96 months**

329 To validate the findings of the above threshold-based analysis and include appropriate adjustments for  
330 potential confounders, all 3 groups were explicitly compared at 42 and 96 months using statistical models.

331 Statistically distinct networks based on the models are shown in Figure 3. No significant gender effects were  
332 found in any parameter at any age ( $p \geq 0.40$ ).

333

#### 334 **3a. Network connectivity**

335 **i) Forty-two months:** Although the above threshold-based analysis identified statistically distinct edges  
336 between the NIG and both the CAUG and FCG, when adjusted for birth weight or head circumference at that  
337 age in the models, no statistically distinct edges were identified between the 3 groups. The effect of age at  
338 foster care placement was found to be significant for right fronto-central (F4, C4) and centro-parietal (C4, P4)  
339 regions in the gamma networks, with statistically higher connections in the CAUG followed by the FCG and  
340 the NIG ( $p = 0.007$ , Wald statistic = 7.74 for group,  $p = 0.006$ , Wald statistic = 7.63 for age at foster care  
341 placement). Connectivity between occipital regions was also statistically higher in the CAUG followed by the  
342 FCG and the NIG and in the alpha and theta networks ( $p = 0.013$ , Wald statistic = 6.39 for group,  $p = 0.027$ ,  
343 Wald statistic = 5.04 for age at foster care placement in the alpha network, and  $p = 0.030$ , Wald statistic = 4.87  
344 for group,  $p = 0.047$ , Wald statistic = 4.07 for foster care placement in the theta network).

345



346 **ii) Ninety-six months:** The majority of aberrantly connected edges identified by the threshold-based analysis  
347 were also found to be distinct in the 3 groups through the statistical models. For oscillations in the gamma to  
348 theta ranges, statistically distinct sub-networks/edges and corresponding brain regions are summarized in  
349 Table 1. Related model statistics for these edges and sub-networks are summarized in Table S3. Adjustments  
350 for birth weight and age at foster care placement were non-significant in all models ( $p > 0.17$  for birth weight  
351 and  $p > 0.06$  for age at placement). Similarly, the adjustment for head circumference was non-significant for all  
352 models for gamma connectivity ( $p > 0.2$ ), all models for beta connectivity with the exception of the (F3, T7)  
353 connectivity ( $p = 0.047$ ) and marginally for the (F4, T7) connectivity ( $p = 0.056$ ), all models for alpha  
354 connectivity with the exception of the (P3, Pz), (P4, Pz) and (T7, O2) connectivities ( $p = 0.028$ ,  $p = 0.019$  and  
355  $p = 0.030$  respectively), and all models for theta with the exception of the (P3, P4) connectivity ( $p = 0.020$  for  
356 theta). Median mutual information for each group is shown in column 2.

357

358 Within the *gamma network*, the parieto-occipital sub-network (P3, Pz, P4, O1, O2 and averaged connectivity  
359 in this subnetwork) was found to be statistically distinct in the 3 groups with highest connectivity in the  
360 CAUG followed by FCG. Elements of this subnetwork were also hyper-connected across frequency ranges.  
361 In the *beta network*, the left temporal region (T7) in the CAUG and FCG was statistically hypo-connected to  
362 several other brain regions, including bilateral frontal (F3, Fz, F4), right temporal (T8), bilateral parietal (P3,  
363 Pz, P4), bilateral occipital (O1, O2) and right central (C4). These connectivities, as well as averaged  
364 connectivity in the corresponding subnetwork were distinct in the 3 groups, with statistically lowest values in  
365 the CAUG. We examined the raw signal from electrode T7 across subjects to ensure that the observed  
366 laterality of these aberrant connectivities was not associated with artifacts or noise. No significant signal  
367 variance differences were found between groups or subjects. All hypo-connections from the beta network were  
368 also found to be distinct between groups in the *alpha network*, with the exception of bilateral frontal, bilateral  
369 temporal and the right central – left temporal connections. Averaged connectivity in this subnetwork was also

370 found to be statistically lowest in the CAUG. In the *theta network*, fronto-parietal (Fz, Pz), bilateral centro-  
371 parietal (C3, P3) and (C4, P4), and most edges of the aberrant gamma subnetwork were statistically distinct  
372 between groups, with highest connectivities in the CAUG followed by the FCG. Also, elements of the hypo-  
373 connected beta subnetwork were distinct in the 3 groups, with lowest connectivities in the CAUG. Finally,  
374 centro-parietal connections in the theta network were also found to be statistically distinct between groups in  
375 the *delta network*, with highest connectivities in the CAUG.

376

### 377 **3b. Node centrality**

378 A few nodes with statistically distinct *connectedness* across the 3 groups were found both at 42 and 96 months  
379 and are summarized in Tables 1 (96 months) and S4 (both ages). At 42 months, these included T7 in the  
380 gamma network; Fz, T7 and T8 in the beta network; Pz in the alpha network; and Fz and Pz in the theta  
381 network. At 96 months, Pz had the highest connectedness in all networks except delta, similarly for C3, C4  
382 and P4 but only in the beta and alpha networks and Fz in the theta network. T7 had the lowest connectedness  
383 in the beta and alpha networks. We examined the raw signals in electrode Pz across subjects to ensure that  
384 increased connectedness was not due to spurious correlations between signals. No significant signal  
385 differences were found between this and other electrodes. Birth weight, head circumference and age at foster  
386 care placement all had a non-significant effects ( $p > 0.08$  for birth weight,  $p > 0.13$  for head circumference and  
387  $p > 0.05$  for age at foster care placement).

388

389 A subset of nodes with distinct connectedness among groups also had distinct *node strengths* but only at 96  
390 months. The statistics of corresponding models are summarized in Table S5. Similarly to connectedness, node  
391 Pz had statistically higher strength in the CAUG in the gamma, beta and alpha networks and node T7 the  
392 lowest strength in the beta to delta networks. Nodes F3, F4, Fz, and T7 all had the lowest strengths in the  
393 CAUG followed by the FCG in the beta network. Finally, P4 was also found to have statistically distinct

394 strength in the 3 groups both in the alpha and theta networks, with highest strength in the CAUG. Birth weight  
395 and age at foster care placement had non-significant effects in all networks and nodes ( $p \geq 0.09$  for both), and  
396 head circumference also had a non-significant effect ( $p \geq 0.08$ ) except for node P4 in the alpha network ( $p =$   
397  $0.016$ ). The spatial distribution of all nodes with distinct strengths in gamma, beta, alpha and theta networks is  
398 shown in Figure 4. In addition to edges that were distinct between groups (those of Figure 3), edges that  
399 exceeded the median (over subjects) NIG connectivity but were not significantly different between groups are  
400 also superimposed (dashed lines). Independently of significance, a higher number of connections were  
401 estimated in the CAUG followed by FCG across oscillations. In summary, a few nodes in previously identified  
402 distinct subnetworks among groups were found to be either aberrant hubs or to have abnormally low centrality  
403 in the CAUG and FCG, suggesting additional topological differences between these groups.

404

#### 405 **4. Network parameter trajectories from 42 to 96 months**

406 All previous analyses investigated network properties at individual assessment ages. To assess the impact of  
407 early neglect on the development of these networks, we also investigated the age-related changes in estimated  
408 parameters from 42 to 96 months using appropriate statistical models for repeated measures.

409

##### 410 **4a. Connectivity trajectories**

411 For each oscillation, the changes in all network edges were estimated and compared between groups, using  
412 mixed effects regression models that included time (age), group and birth weight or head circumference  
413 (and/or age at foster care placement) as independent variables and pairwise MI as the dependent connectivity  
414 variable. The statistics of these models for edges that were distinct between groups are summarized in Table  
415 S6a. The effect of time (age) was significant in all these models ( $p \leq 0.01$ ). Birth weight, and head  
416 circumference had non-significant effects in all models ( $p > 0.17$  for birth weight,  $p > 0.26$  for circumference).  
417 A small number of network connections had distinct age-related changes across groups, including (P3, Pz) and

418 (P4, O2) across oscillations except delta, and (C3, P3), (P3, O2), (P4, O1) and (Pz, O2) in the gamma network.  
419 Note that with the exception of (C3, P3) these edges were also found to be distinct at 96 months and were part  
420 of the parieto-occipital hyper-connected subnetwork in the CAUG and FCG compared to NIG.

421

#### 422 **4b. Node centrality**

423 With the exception of node P3 in the gamma network with marginally significant age-related changes across  
424 groups ( $p = 0.053$ , Wald statistic = 3.77) no other node strength changed significantly from 42 to 96 months.  
425 However, connectedness in nodes P4 and Pz in the alpha and theta networks changed in a statistically distinct  
426 way across groups. Both nodes belong to the subset of nodes with distinct connectedness at 96 months in the 3  
427 groups (Pz also had statistically distinct connectedness at 42 months; see Table S6b). Birth weight and head  
428 circumference had non-significant effects ( $p > 0.21$  for birth weight,  $p > 0.05$  for head circumference). These  
429 results suggest that at least elements (nodes and edges) of task-independent networks develop abnormally as a  
430 function of age in children reared in institutions, resulting in significant differences at 96 months.

431 **Discussion**

432 In this paper we report the impact of early psychosocial deprivation associated with institutionalization on the  
433 topologies and age-related dynamics of frequency (oscillation)-specific, task-independent brain networks in  
434 three groups of children from the BEIP. To investigate these topologies, we have used multiple statistical  
435 modeling approaches and network measures. Our present findings extend previous work (Stamoulis et al,  
436 2015), which has shown that early institutionalization has profound and widespread effects on broadband  
437 neural activity.

438

439 In children reared in institutions and thus subjected to early neglect, this study has identified two aberrantly  
440 connected networks, particularly at 96 months: 1) the *aberrantly hyper-connected parieto-occipital gamma*  
441 *network* in the CAUG and FCG, both with statistically higher connectivity than the NIG, but also with  
442 distinctly different connectivity from each other. Elements of this subnetwork were also aberrantly hyper-  
443 connected at lower frequencies (beta, alpha and theta networks); 2) the *hypo-connected fronto-temporal*  
444 *network* at frequencies below the gamma range (beta to delta) in the CAUG and FCG compared to NIG at 96  
445 months, but also distinctly different from each other. Although the adverse effects of early stressors on neural  
446 maturation and the development of human brain networks remain elusive, there is substantial evidence that  
447 brain development is significantly impacted by early experiences (Nelson et al, 2006). Therefore, negative  
448 experiences may significantly and differentially affect the maturation of the brain's neural circuitry, impairing  
449 both selective connection strengthening (leading to hypo-connected networks), and/or connection pruning  
450 (leading to networks that appear aberrantly hyper-connected at the macroscale). Both types of aberrant  
451 networks may prevent efficient neural information processing.

452

453 It is important to note the statistically lower connectivity in the FCG (although still statistically higher than  
454 NIG) compared to CAUG in the parieto-occipital network, suggesting a positive effect of the foster care

455 intervention in lowering aberrant hyper-connectivity. Previous work has shown that this network is  
456 synchronized in the gamma band during visual processing (Helfrich et al, 2014). Abnormally high  
457 connectivity may imply reduced flexibility of this network to modulate its activity during visual task  
458 performance. In fMRI studies, elements of this network have been previously identified as major cortical hubs  
459 (Tomasi et al., 2011). Here, parietal nodes, which may overlap with this network, were found to be aberrant  
460 hubs at multiple frequencies, with abnormally high connectivities in the CAUG and FCG compared to the  
461 NIG. These regions are involved in a wide range of cognitive processes. For example, parietal regions are  
462 often activated during episodic memory retrieval (Cabeza, et al 2008) and are involved in self-projection  
463 (Buckner et al., 2007) as well as visuo-spatial processing (Tosoni et al, 2014). Furthermore, spatial attention  
464 has been shown to modulate the coordination between parietal and occipital regions during top-down  
465 processing of spatial attention information (Lauritzen et al., 2009). Thus, abnormally high task-independent  
466 connectivity between these areas may adversely impact these cognitive processes.

467

468 Although elements of the hyper-connected parieto-occipital network had distinct connectivities in the 3 groups  
469 across frequencies, the largest number of aberrant edges in this subnetwork was estimated in the gamma  
470 frequency range. Gamma synchrony in parietal regions has been associated with visuo-motor learning and  
471 object representation (e.g., Bertrand et al., 2000; Perfetti et al., 2001; Galletti et al., 2003; Tallon-Baudry,  
472 2009). Previous studies have shown that children reared in institutions have decreased performance on tests of  
473 visual memory and attention (Bos et al., 2009; Pollack et al, 2010; Bick et al., in press), which may be  
474 explained by decreased flexibility in the underlying neural circuitry. At lower frequencies, particularly the  
475 theta and delta ranges, fronto-parietal regions, which appeared to be aberrantly hyper-connected in the CAUG  
476 and FCG, have been shown to be part of a network that is characterized by spontaneous low-frequency activity  
477 and is anti-correlated with the DMN (Fox et al., 2005; Konrad et al., 2010), which implies that it should be  
478 weakly correlated at rest, in contrast to the DMN. Although neuronal networks identified in this study with

479 low spatial resolution-EEG are not directly comparable with high-resolution fMRI networks, similar anti-  
480 correlations between task-dependent and task-independent networks may be measurable by both modalities.  
481 Therefore, aberrantly high task-independent connectivity in the identified parieto-occipital network may  
482 prevent suppression of its resting activity and inhibit its functional activation.  
483

484 The second major finding of this study is the *hypo-connected fronto-temporal network* at frequencies below  
485 the gamma range (beta to delta) in the CAUG and FCG compared to NIG at 96 months. Several elements of  
486 this network may overlap with previously identified task-independent networks, e.g., the resting-state  
487 auditory-phonological and visual networks reported by Mantini et al. (2007). Left middle and transverse  
488 temporal regions, covered by electrode T7, were found to be significantly hypo-connected with bilateral  
489 frontal (F3, Fz, F4), bilateral occipital (O1, O2) and right temporal (T8) regions. This node was also found to  
490 have statistically lower important (centrality) in the network in the CAUG and FCG. Left temporal regions are  
491 associated with hearing, language processing and memory. The parietal-temporal-occipital association area is  
492 responsible for integrating visual and auditory information and is involved in language comprehension. Left  
493 fronto-temporal connectivity has also been shown to be an essential network involved in syntactic processing  
494 (Tyler et al, 2011; Papoutsi et al, 2011). Note that spatially-averaged connectivity in the left hemisphere was  
495 also found to be distinct in the 3 groups at 96 months, in the beta and theta networks. Again, our findings may  
496 tap an underlying aberrant network associated with the behavioral evidence of impaired language development  
497 as a result of early institutionalization. It is important to note the distinct connectivity in this subnetwork in the  
498 CAUG and FCG, suggesting a positive effect of the foster care intervention in increasing connectivity in this  
499 subnetwork. Thus, this change could be associated with the observed improvements in language learning as a  
500 result of the foster care intervention and age of that intervention (Croft et al., 2007; Windsor et al, 2011, 2013).  
501 A previous study of structural brain connectivity in the BEIP cohort (Bick et al, 2015) has shown impaired  
502 integrity of the corpus callosum in children reared in institutions, which would in part explain lower inter-

503 hemispheric connectivity between temporal regions in the CAUG and FCG.  
504

505 Although all network analyses in this study have consistently identified both the hyper-connected parieto-  
506 occipital network and the hypo-connected primarily left temporal network across several frequency bands at  
507 96 months, corresponding findings at 42 months were less clear. A few elements of the parieto-occipital  
508 subnetwork with aberrant characteristics at 42 months remained atypically connected at 96 months, with  
509 distinct properties in the 3 groups. The dynamic trajectories of part of this subnetwork were also distinct  
510 among groups, potentially due to differential neural maturation rates. It is possible that additional network  
511 differences were difficult to detect at 42 months due to incomplete and heterogeneous maturation of task-  
512 independent networks at this age, which could make it more difficult to detect connectivity group differences.  
513

514 Finally, the frequency specificity of our findings varied between networks (e.g., a larger hyper-connected  
515 network in the gamma range compared to lower frequencies). Although higher-frequency networks imply  
516 spatially localized processing, lower-frequency oscillations facilitate the communication (or binding) between  
517 these networks. The presence of smaller numbers of aberrant connections at lower frequencies could in part be  
518 due to impaired binding between high- and lower-frequency oscillations within corresponding networks. Our  
519 previous work has shown decreased coupling between task-independent gamma and lower-frequency  
520 oscillations, which could in part explain these findings (Stamoulis et al., 2015). Furthermore, substantial  
521 topological overlap between aberrantly hypo-connected edges were observed in the alpha and beta networks.  
522 Significant correlations between alpha and beta oscillations have been reported in task-independent EEGs,  
523 which may explain the topological similarities between the two networks (Carlqvist et al., 2005).  
524

525 Despite its many methodological strengths (including its randomized control trial design), this study is not  
526 without limitations, including its relatively small sample size. Nevertheless, data from multiple time points



527 were included in parts of the statistical analysis, and multiple statistical models were developed to compare the  
528 cohorts, all yielding consistent results, which supports the robustness of the findings. It is, however, possible  
529 that smaller network-level differences between groups were not detectable in this sample. Second, a small  
530 number of electrodes was used to record brain activity, which prevented appropriate source-level analyses to  
531 explicitly address the issue of volume conduction. However, information-based measures of connectivity were  
532 used in this study, which have been previously been shown to be relatively robust to volume conduction. Also,  
533 the low spatial resolution of the EEG limits the estimation of detailed network topologies possible by other  
534 modalities, particularly fMRI. Despite these limitations, to the best of our knowledge, this study provides the  
535 first evidence of multiple, significantly impacted and aberrantly connected task-independent brain networks in  
536 children who have experienced severe psychosocial deprivation. Considering these networks' potential  
537 involvement in cognitive processing, including memory, visuo-motor learning, visual processing, social  
538 communication and language, these findings suggest that early psychosocial neglect associated with  
539 institutionalization may have profound adverse effects on the brain's wiring and communication, which may  
540 not be fully reversible, at least not within a few years from the intervention. Nevertheless, statistical  
541 differences between the CAUG and FCG also suggest significant positive effects of foster care on improving  
542 neural information processing facilitated by these networks.

543

#### 544 **Funding**

545 This study was supported in part by NIH Grant R01MH091363 (Nelson) and NSF BRAIN EAGER Grant  
546 1451480 (Stamoulis).

547 **References**

548

549 [1] Andreou, C, Nolter, G, Leight, G, Polomac, N, Hanganu-Opatz IL, Lambert, M, Engel, AK, Mulert, C  
550 (2015), Increased Resting-State Gamma-Band Connectivity in First-Episode Schizophrenia, *Schizophr Bull*,  
551 41(4):930-939.

552

553 [2] Bauer PM, Hanson JL, Pierson RK, Davidson RJ, Pollak SD (2009) Cerebellar volume and cognitive  
554 functioning in children who experienced early deprivation, *Biol Psychiatry* 66: 1100–1106.

555

556 [3] Barttfeld, P, Uhrig, L, Sitt, JD, Sigman, M, Jarraya, B, Dehane, S (2015), Signature of consciousness in  
557 the dynamics of resting-state activity, *Proc Nat Acad Sci* , 112(3): 887-892.

558

559 [4] Bertrand, O, Tallon-Baudry, C (2000) Oscillatory gamma activity in humans: a possible role for object  
560 representation, *Int J Psychophysiol*, 38(3): 211-223.

561

562 [5] Bick, J., Zhu, T., Stamoulis, C., Fox, NA, Zeanah, C., Nelson, CA (2015), Effect of Early  
563 Institutionalization and Foster Care on Long-term White Matter Development: A Randomized Clinical Trial,  
564 *JAMA Pediatr*, 169(3): 211-9.

565

566 [6] Bick, J, Zeanah CH, Fox NA, & Nelson CA (in press). Memory and executive functioning in 12-Year-Old  
567 children with histories of institutional rearing. *Child Development*.

568

569 [7] Bluhm, RL, Miller, J, Lanius, RA, Osuch, EA, Boksman, EA (2007), Spontaneous low-frequency  
570 fluctuations in the BOLD signal in schizophrenia patients: anomalies in the default networks, *Schizophr. Bull.*,

571 33: 1004-1012.

572

573 [8] Bos, K, Zeanah, CH, Fox, NA, Drury, SS, McLaughlin, KA, Nelson CA (2011), Psychiatric Outcomes in  
574 Young Children with a History of Institutionalization, *Harv Rev Psychiatry*, 19(1): 15–24.

575

576 [9] Bos K, Fox NA, Zeanah CH, & Nelson CA (2009), Effects of early psychosocial deprivation on the  
577 development of memory and executive function. *Frontiers in Behavioral Neuroscience*, 3:16.

578

579 [10] Buckner, RL, Carroll, DC (2007), Self-projection and the brain, *Trends Cogn Sci*, 11: 49-57.

580

581 [11] Buckner, RL, Andrews-Hanna, JR, Schachter, DL (2008), The brain's default network: anatomy, function,  
582 and relevance to disease, *Ann NY Acad Sci*, 1124: 1-38.

583

584 [12] Bullmore, E., Sporns, O (2009), Complex brain networks: graph theoretical analysis of structural and  
585 functional systems, *Nat Rev Neurosci*, 10(3):186-98.

586

587 [13] Carey, PD, Warwick, J, Niehaus, DJ, van der Linden, G, van Heerden, BB, Harvey, BH, Seedat, S., Stein,  
588 DJ (2004), Single photon emission computed tomography (SPECT) of anxiety disorders before and after  
589 treatment with citalopram. *BMC Psychiatry* 4, 30.

590

591 [14] Cabeza, R, Ciaramelli, E, Olson, IR, Moscovitch, M (2008), Parietal cortex and episodic memory: an  
592 attentional account, *Nat Rev Neurosci*, 9(8): 613-625.

593

594 [15] Calqvist, H, Nikulin, VV, Stromberg, JO, Brismar, T (2005), Amplitude and phase relationship between

595 alpha and beta oscillations in the human electroencephalogram, *Med Biol Eng Comput*, 43(5):599-607.

596

597 [16] Chella, F, Pizzella, V, Zappasodi, F, Marzetti, L (2016), Impact of the reference choice on scalp EEG

598 connectivity estimation, *J Neural Eng*, 13: 1-21.

599

600 [17] Chugani HT, Behen ME, Muzik O, Juhasz C, Nagy F, et al. (2001) Local brain functional activity

601 following early deprivation: A study of post-institutionalized Romanian orphans. *NeuroImage* 14: 1290–1301.

602

603 [18] Croft, C, Beckett C, Rutter M, Castle J, Colvert E, Groothues C, et al (2007). Early adolescent outcomes

604 of institutionally deprived and non-deprived adoptees. II: Language as a protective factor and a vulnerable

605 outcome. *J Child Psychol Psychiatry*, 48:31–44.

606

607 [19] Courchesne, E., Pierce, K (2005), Why the frontal cortex in autism might be talking only to itself: local

608 over-connectivity but long-distance disconnection, *Curr Op Neurobiol*, 15: 225-230.

609

610 [20] Dien, J (1998), Issues in the application of the average reference: Review, critiques, and

611 recommendations, *Behavior Research Methods. Instruments. & Computers*, 30 (1). 34-43.

612

613 [21] Dosenbach, NU, Fair, DA, Cohen, AL, Schlaggar, BL, Petersen, SE (2008), A dual-networks architecture

614 of top-down control, *Trends Cogn Sci*, 12(3): 99–105

615

616 [22] Efron, B, Tibshirani, R (1993), An introduction to the bootstrap, New York: Chapman and Hall

617

618 [23] Fair DA, Cohen AL, Dosenbach NU, Church JA, Miezin FM, Barch DM, Raichle ME, Petersen SE,

619 Schlaggar BL (2008), The maturing architecture of the brain's default network. *Proc Natl Acad Sci USA*  
620 105:4028–4032.

621

622 [24] Fox, Snyder AZ, Vincent JL, Corbetta M, Van Essen DC, Raichle ME (2005): The human brain is  
623 intrinsically organized into dynamic, anti-correlated functional networks. *Proc Natl Acad Sci USA* 102:9673–  
624 9678.

625

626 [25] Fransson, P, Skold, B, Horsh, S, Nordell, A, Blennow, M, Lagercrantz, H, Aden, U (2007) , Resting-  
627 state networks in the infant brain, *Proc Nat Acad Sci*, 104(39): 15531–15536.

628

629 [26] Galletti, C, Kutz, DF, Gamberini, M, Breveglieri, R, Fattori, P (2003), P, Role of the medial parieto-  
630 occipital cortex in the control of reaching and grasping movements, *Exp Brain Res* 153(2):158-170.

631

632 [27] Gelman, A, Hill, J, Yajima, M (2012), Why we (usually) don't have to worry about multiple comparisons,  
633 *J Res Educ Eff*, 5: 189-211.

634

635 [28] Gentili, C., Ricciardi, E., Gobbini, MI., Santarelli, MF., Haxby, JV., Pietrini, P., Guazzelli, M (2009),  
636 Beyond amygdala: Default Mode Network activity differs between patients with social phobia and healthy  
637 controls. *Brain Res. Bull.* 79: 409–413

638

639 [29] Greicius, MD, Krasnow, B, Reiss, AL, Menon, V (2003), Functional connectivity in the resting brain: A  
640 network analysis of the default mode hypothesis, *Proc Natl Acad Sci* (100): 253-258.

641

642 [30] Greicius, MD, Flores, BH, Menon, V, Glover, GH, Solvason, HB, Kenna, H, Reiss, AL, Schatzberg, AF

643 (2007), Resting-state functional connectivity in major depression: abnormally increased contributions from  
644 subgenual cingulate cortex and thalamus, *Biol Psychiatry*, 62(5): 429-437.

645

646 [31] Greicius, MD, Supekar, K, Menon, V, Dougherty, RF (2009), Resting-state functional connectivity  
647 reflects structural connectivity in the default mode network, *Cerebr Cort* 19: 72-78.

648

649 [32] Helfrich RF, Knepper H, Nolte G, Strüber D, Rach S, (2014) Selective modulation of inter-hemispheric  
650 functional connectivity by HD-tACS shapes perception. *PLoS Biol* 12: e1002031

651

652 [33] Huang, NE, Shen, Z, Long, SR, Wu, MC, Shih, HH, Zheng, Q, Yen, NC, Tung, CC, Liu, HH (1998)  
653 The empirical mode decomposition and the Hilbert spectrum for nonlinear and non-stationary time series  
654 analysis, *Proc Royal Soc A*, 454 (1971): 903–995.

655

656 [34] Kelly, C, Uddin, LQ, Biswal, BB, Castellanos, FX, Milham, MP (2008), Competition between functional  
657 brain networks mediates behavioral variability, *Neuroimage*, (39): 527-537.

658

659 [35] Kennedy, DP, Courchesne, E (2008) Failing to deactivate: resting functional abnormalities in autism, *Proc*  
660 *Natl Acad Sci*, 103: 8275-8280.

661

662 [35] Konrad, K, Eickhoff, SB (2010) Is the ADHD Brain Wired Differently? A Review on Structural and  
663 Functional Connectivity in Attention Deficit Hyperactivity Disorder, *Hum Brain Mapp*, 31(6):904-16.

664

665 [36] Levin, AR, Fox, NA, Zeanah, CH, Nelson CA (2015), Social communication difficulties and autism in  
666 previously institutionalized children, *J Am Acad Child Adolesc Psychiatry*, 54(2): 108-115.

667

668 [37] Lauriten, TZ, D'Esposito, M, Heeger, DJ, Solver, MA, Top-down flow of visual spatial attention signals  
669 from parietal to occipital, *Journal of Vision* 9(13): 1-14.  
670

671 [38] Liao, W, Chen, H, Feng, Y, Mantini, D, Gentili, C, Pan, Z, Ding J, Duan, X, Qiu, C, Liu, S, Gong, Q,  
672 Zhang, W (2010) Selective aberrant functional connectivity of resting state networks in social anxiety  
673 disorder, *Neuroimage*, 52: 1549–1558.  
674

675 [39] Marshall, PJ, Reeb, BC, Fox, NA, Nelson CA, Zeanah CH (2008) Effects of early intervention of EEG  
676 power and coherence in previously institutionalized children in Romania, *Dev Psychopathol.*, 20(3):861-80.  
677

678 [40] Marshall PJ, Fox NA and Bucharest Early Intervention Project Core Group, A comparison of the  
679 electroencephalogram between institutionalized and community children in Romania (2004), *J Cogn  
680 Neurosci.*, 16(8):1327-38.  
681

682 [41] McLaughlin, KA, Fox, NA, Zeanah, CH, Sheridan MA, Marshall, P, Nelson CA (2010), Delayed  
683 maturation in brain electrical activity partially explains the association between early environmental  
684 deprivation and symptoms of attention-deficit/hyper-activity disorders, *Biol Psychiatry*, 15:68(4): 239-336.  
685

686 [42] McLaughlin, KA, Fox, NA, Zeanah, CH, Sheridan MA, Nelson CA (2011) Adverse rearing environments  
687 and neural development in children: the development of frontal electroencephalogram asymmetry, *Biol  
688 Psychiatry*, 70:1008-1015  
689

690 [43] Nelson, CA, Fox, Na, Zeanah, CH (2014), *Romania's abandoned children: Deprivation, brain  
691 development and the struggle for recovery*, Cambridge, MA, Harvard University Press.

692

693 [44] Nelson, CA, de Haan, M, Thomas, KM (2006), *Neuroscience of Cognitive Development: The Role of*  
694 *Experience and the Developing Brain*, Wiley, NY.

695

696 [45] Nickl-Jockschat, Rottschy, C, Thommes, J, Schneider, F, Laird, AR, Fox, PT, Eickhoff, SB (2015), *Neural*  
697 *networks related to dysfunctional face processing in autism spectrum disorder*, *Brain Struct Func*, 220(4):  
698 2355-237

699

700 [46] Northam, GB, Liegeois, F, Tournier, JD, Croft, LJ, Johns, PN, Ching, WK, Wyatt, JS, Baldeweg, T  
701 (2012), *Inter-hemispheric temporal lobe connectivity predicts language impairment in adolescents born*  
702 *preterm*, *Brain*, 135(Pt 12):3781-3798.

703

704 [47] Palus, M, Komarek, V, Prochazka, T, Hrnčir, Z, Sterbova, K (2001), *IEEE Eng. Med. Biol. Mag*,  
705 20(5):65-71.

706

707 [48] Papoutsis, M, Stamatakis, EA, Griffiths, J, Marslen-Wilson WD, Tyler, LK(2011) *Is left fronto-temporal*  
708 *connectivity essential for syntax? Effective connectivity, tractography and performance in left-hemisphere*  
709 *damaged patients*, *Neuroimage*, 58(2):656-64

710

711 [49] Perfetti, B, Moisello, C, Landsnesors, EC, Kvint, S, Lanzafame, S, Onofri, M, Di Rocco, A, Tononi, G,  
712 Ghilardi, MF (2011), *Modulation of gamma and theta spectral amplitude and phase synchronization is*  
713 *associated with the development of visuo-motor learning*, *J Neurosci*, 31(41): 14810-14819.

714

715 [50] Pollack, S, Nelson, CA, Schlaak, MF, Roeber, BJ, Wewerka, SS, Wilk, KL, Frenn, KA, Loman, MM,



716 Gunnar, MR, Neurodevelopmental effects of early deprivation in post-institutionalized children, *Child Dev*  
717 81(1): 224- 236.

718

719 [51] Raichle, ME, MacLeod, AM, Snyder, AZ, Powers, WJ, Gusnard, DA, Shulman, GL (2001), A default  
720 mode of brain function. *Proc Natl Acad Sci*, (98):676–682.

721

722 [52] Raichle, ME., Snyder, AZ (2007), A default mode of brain function: a brief history of an evolving idea,  
723 *NeuroImage* 237:1083–1090.

724

725 [53] Schreiber, T (2000), Measuring information transfer, *Phys. Rev. Lett.*, 85(2):461-464.

726

727 [54] Sheridan MA, Fox NA, Zeanah CH, McLaughlin KA, Nelson CA (2012), Variation in neural  
728 development as a result of exposure to institutionalization early in childhood, *Proc Nat Acad Sci*,  
729 109(32):12927-32.

730

731 [54] Stamoulis, C, Chang, BS (2009)., Application of matched-filtering to extract EEG features and decouple  
732 signal contributions from multiple seizure foci in brain malformations, *IEEE Proc 4th International*  
733 *IEEE/EBMS Conf Neural Eng*, 514-517.

734

735 [55] Stamoulis, C., Betensky, RA (2011), A novel signal processing approach for the detection of copy-number  
736 variations in the human genome, *Bionformatics*, 27(17):2338-2345.

737

738 [55] Stamoulis, C., Schomer, D.L., Chang, B.S (2013), Information theoretic measures of network  
739 coordination in high-frequency scalp EEG reveal dynamic patterns associated with seizure termination,

740 *Epilepsy Res.* 105(3):299-315.

741

742 [56] Stamoulis, C., Vanderwert, RE, Zeanah, CH, Fox, NA, Nelson, CA (2015), Early psychosocial

743 deprivation adversely impacts developmental trajectories of brain rhythms and their interactions, *J Cogn*

744 *Neurosci*, 27(12): 2512-2528.

745

746 [57] Stamoulis, C, Vogel-Farley, V. Degregorio, G., Jeste, SS., Nelson, C.A (2014), Resting and Task-

747 Modulated High-Frequency Brain Rhythms Measured by Scalp Encephalograms in Infants with Tuberous

748 Sclerosis Complex, *J Autism Develop Disord*, 45(2):336-532014.

749

750 [58] Tallon-Baudry, C (2009), The roles of gamma-band oscillatory synchrony in human visual cognition

751 *Front Biosci*, 14: 321-332.

752

753 [59] Tomasi, D, Volkow, ND (2011), Association between functional connectivity hubs and brain networks,

754 *Cereb Cortex*, 21(9): 2003-2013.

755

756 [60] Tononi, J., Sporns, O., Edelman, GM (1994), A measure for brain complexity: Relating functional

757 segregation and integration in the nervous system, *Proc Natl Acad Sci* (91): 5033-5037.

758

759 [61] Tosoni, A, Pitzalis, S, Committeri, G, Fattori, P, Galletti, C, Galati, G (2015), Resting-state connectivity

760 and functional specialization in human medial parieto-occipital cortex, *Brain Struct Func*, 220(6): 3307-3321.

761

762 [62] Tottenham, N, Hare, TA, Millner, A, Gilhooly, T, Zevin, JD, Casey, BJ (2011), Elevated amygdala

763 response to faces following early deprivation, *Dev Sci*, 14(2): 190-204.

764

765 [63] Tukey, JW (1977) Exploratory data analysis, Addison-Wesley.

766

767 [64] Tyler, LK, Marslen-Wilson, WD, Randall, B, Devereaux, BJ, Zhuand, J, Papoutsis, M, Stamatakis, EA  
768 (2011) Left inferior frontal cortex and syntax: function, structure and behavior in patients with left hemisphere  
769 damage, *Brain*, 134(Pt 2):415-31.

770

771 [65] Vanderwert RE, Marshall PJ, Nelson CA 3rd, Zeanah CH, Fox NA (2010), Timing of Intervention Effects  
772 Affects Brain Electrical Activity in Children Exposed to Severe Psychosocial Neglect, *PloS One*, 5(7):  
773 e11415.

774

775 [66] Vejmelka, M, Palus, M (2008), Inferring the directionality of coupling with conditional mutual  
776 information, *Phys. Rev. E*, 77:026214.

777

778 [67] Vicente, R., Wibral M., Lindner M., Pipa G. (2011). Transfer entropy—a model-free measure of effective  
779 connectivity for the neurosciences. *J. Comput. Neurosci.* 30, 45–67.

780

781 [68] Vincent, JL, Snyder, AZ, Fox, MD, Shannon, BJ, Andrews, JR, Raichle, ME, Buckner, RL (2006),  
782 Coherent spontaneous activity identifies a hippocampal–parietal memory network. *J. Neurophysiol*, 96, 3517–  
783 3531

784

785 [69] Ward, AM, Schultz, AP, Huijbers, W, Van Dijk, KR, Hedden, T, Sperling, RA (2014), The  
786 parahippocampal gyrus links the default-mode cortical network with the medial temporal lobe memory  
787 system, *Hum Brain Mapp*, 35(3): 1061-1073.

788

789 [70] Warwick, JM, Carey, P, Jordaan, GP, Dupont, P, Stein, DJ (2008), Resting brain perfusion in social  
790 anxiety disorder: a voxel-wise whole brain comparison with healthy control subjects. *Prog.*  
791 *Neuropsychopharmacol. Biol. Psychiatry* 32: 1251–1256.

792

793 [71] Widom CS, DuMont K, Czaja SJ (2007). A prospective investigation of major depressive disorder and co-  
794 morbidity in abused and neglected children grown up. *Arch Gen Psychiatry*, 64:49–56.

795

796 [72] Windsor J, Benigno JP, Wing CA, Carroll PJ, Koga SF, Nelson CA 3rd, Fox NA, Zeanah CH (2011),  
797 Effects of foster care on young children's language learning, *Child Dev*, 82(4):1040-6.

798

799 [73] Windsor, J, Morary, A, Nelson, CA, Fox, NA, Zeanah, CH (2013), Effect of foster care on language  
800 learning at eight years: findings from the Bucharest Early Intervention Project, *J Child Lang*, 40(3):605-27.

801

802 [74] Wu, Z, Huang, N (2009), Ensemble Empirical Mode Decomposition: A Noise Assisted Data Analysis  
803 Method, *Advances in Adaptive Data Analysis*, 1-41, World Scientific Publishing Company.

804

805 [75] Zeanah, CH, Nelson CA, Fox NA, Smyke, AT, Marshall, PJ, Parker, SW, Koga, S (2003) Designing  
806 research to study the effects on institutionalization on brain and behavioral development: The Bucharest Early  
807 Intervention Project, *Dev Psychopathol*, 15:885-907.

808

809

810

811

812

813  
814  
815  
816

## **Tables**

<b>Oscillation/Network</b>	<b>Edge Connectivity</b>		<b>Node Centrality</b>	
	<b>Hyper-connected</b>	<b>Hypo-connected</b>	<b>Highest</b>	<b>Lowest</b>
Gamma-range (52.0-57.0 Hz)	<b><u>Regions:</u></b> Parietal; Parieto-occipital	–	Pz	
	<b><u>Edges:</u></b> P3-Pz; P4-O1, O2; Pz-O1,O2			
Beta-range (20.0-23.0 Hz)	<b><u>Regions:</u></b> Parietal	<b><u>Regions:</u></b> Left temporal; Bilateral frontal; Parietal; Occipital	Pz, C3, C4, P4	T7, F3, F4, Fz
	<b><u>Edges:</u></b> P3-Pz	<b><u>Edges:</u></b> T7-F3, Fz, F4, C4, P3, Pz,P4, O1, O2; F3-F4; T7-T8		
Alpha-range (8.0-10.0 Hz)	<b><u>Regions:</u></b> Parietal; Parieto-occipital	<b><u>Regions:</u></b> Left temporal; Bilateral frontal; Parietal; Occipital	Pz, C3, C4, P4	T7
	<b><u>Edges:</u></b> P3-Pz, P4-Pz, P4- O2	<b><u>Edges:</u></b> T7-F3, Fz,F4, C4, P3, Pz,P4, O1, O2		
Theta-range (3.6-4.3 Hz)	<b><u>Regions:</u></b> Midline; Centro-parietal; Parietal; Parieto-occipital	<b><u>Regions:</u></b> Left, bilateral temporal; Bilateral Centro-parietal; Parietal; Occipital	Pz, Fz, C3, C4, P4	T7
	<b><u>Edges:</u></b> Fz-Pz, C3-P3, C3-P4, O1-O2, P3-P4, P4-O1, P4-O2, P3-Pz	<b><u>Edges:</u></b> Fz-T7, Pz; C3-P3, C4-P4, P3-Pz, P4; P4-O1,O2; T7-T8; O1- O2		

817

818 **Table 1:** Summary of aberrantly connected and statistically distinct network elements (edges and nodes) in the  
819 three groups. For each oscillation frequency range, hyper- and hypo-connected brain regions and sets of  
820 network edges as well as aberrantly connected nodes (based on their centrality estimated either as node  
821 strength or connectedness) are listed.

822

823

824

825

826

827

828 **Figures Legends**

829 **Figure 1:** Frequency-connectivity (measured by mutual information) plots for all estimated oscillations at  
830 baseline (top left panel), and clockwise at ~30-33, 42, and 96 months respectively. At the first 3 time points  
831 connectivity was estimated from task-independent EEGs under the lights off recording condition and at 96  
832 months under the eyes-closed condition. The 3 groups are superimposed: Care as Usual group (CAUG, red),  
833 Foster Care group (FCG, blue) and Never Institutionalized group (NIG, black). At baseline, and thus prior to  
834 randomization, children in the CAUG and FCG were part of the 'Institutionalized' group.

835

836 **Figure 2:** Hyper- and hypo-connected network edges and subnetworks in the CAUG and FCG relative to the  
837 NIG, for each estimated oscillation and at each assessment age (baseline to 96 months from left to right).  
838 Edges with mutual information (MI) values higher than the upper MI threshold are marked in red, and edges  
839 with MI values below the lower MI threshold are marked in green.

840

841 **Figure 3:** Oscillation-specific network edges for which connectivity was statistically distinct in the 3 groups,  
842 adjusted for birth weight and head circumference at each age. Left panel plots correspond to the CAUG (red),  
843 middle panels to the FCG (blue) and right panels to the NIG (black). Distinct line widths represent differential  
844 median (across the group) mutual information values, with thickest lines representing the highest median  
845 connectivity among groups and the thinnest lines representing the lowest connectivity.

846

847 **Figure 4:** Network nodes with aberrant strength (centrality) across groups, in the gamma, beta, alpha and theta  
848 networks. Larger circles and thicker lines reflect aberrantly and significantly higher node strength and  
849 connectivity (edge weight). Dashed lines correspond to edges above the NIG median connectivity threshold,  
850 which were not, however, statistically distinct between groups. Colors correspond to individual groups  
851 (CAUG - red, FCG - blue and NIG - black).

852 **Supplemental Material**

853

Assessment	Baseline		42 months		96 months	
Group	Median % time; Actual time (months)	(25 <sup>th</sup> , 75 <sup>th</sup> ) quartiles	Median time; Actual time (months)	(25 <sup>th</sup> , 75 <sup>th</sup> ) quartiles	Median time; Actual time (months)	(25 <sup>th</sup> , 75 <sup>th</sup> ) quartiles
CAUG	98.6% 19 mo	(81.6, 100.0)% (16.9, 25.0) mo	85.0% 35.7 mo	(64.4, 97.1)% (27.0, 40.8) mo	53.0% 50.9 mo	(36.2, 79.8)% (31.2, 67.6) mo
FCG	95.9% 18.3 mo	(69.4, 100.0)% (16.3, 23.0) mo	48.9% 20.5 mo	(35.0, 61.8) % (14.7, 26.0) mo	23.40% 22.5 mo	(18.3, 28.6)% (15.0, 26.5) mo
NIG	0	0	0	0	0	0

854

855

856 **Table S1:** Summary statistics of percent time since birth spent in institutions and corresponding time in

857 months, for each group at baseline, 42 and 96 months.

858

859

860

861

862

863

864

865

866

867

868

869

870

871

872

873

874

875

876

877

878

879

880

881

882

883

884

885

886

Age (months)	Band range	Care as Usual Group		Foster Care Group		Never-Institutionalized Group	
		Median (Hz)	(25 <sup>th</sup> , 75 <sup>th</sup> ) quartiles	Median (Hz)	(25 <sup>th</sup> , 75 <sup>th</sup> ) quartiles	Median (Hz)	(25 <sup>th</sup> , 75 <sup>th</sup> ) quartiles
Baseline (< 30)	Gamma	51.82	(49.93, 53.65)	50.89	(49.71, 51.82)	49.12	(48.21, 50.35)
	Beta	20.57	(19.27, 21.30)	20.18	(19.58, 20.89)	19.82	(18.87, 20.21)
	Alpha	8.24	(7.85, 8.58)	8.23	(7.96, 8.56)	8.14	(7.87, 8.45)
	Theta	3.55	(3.42, 3.69)	3.61	(3.43, 3.70)	3.61	(3.46, 3.72)
	Delta	1.54	(1.46, 1.59)	1.56	(1.47, 1.61)	1.56	(1.50, 1.61)
30-33	Gamma	50.14	(48.41, 52.47)	51.34	(48.84, 53.69)	50.01	(48.44, 53.24)
	Beta	19.94	(18.79, 21.11)	20.47	(19.39, 21.70)	19.78	(18.55, 21.47)
	Alpha	8.20	(7.73, 8.64)	8.43	(7.92, 8.88)	8.28	(7.86, 8.82)
	Theta	3.60	(3.40, 3.79)	3.66	(3.42, 3.95)	3.64	(3.47, 3.85)
	Delta	1.54	(1.45, 1.63)	1.58	(1.49, 1.72)	1.60	(1.51, 1.64)
42	Gamma	52.96	(50.16, 55.25)	53.55	(50.59, 56.54)	53.14	(48.20, 56.59)
	Beta	20.58	(19.46, 22.01)	21.47	(19.70, 22.62)	21.34	(18.56, 22.88)
	Alpha	8.54	(8.13, 9.04)	8.69	(8.30, 9.32)	8.81	(8.17, 9.58)
	Theta	3.71	(3.56, 3.96)	3.82	(3.58, 4.14)	3.90	(3.62, 4.25)
	Delta	1.60	(1.52, 1.70)	1.65	(1.51, 1.80)	1.69	(1.56, 1.83)
96	Gamma	55.54	(53.19, 57.20)	54.34	(52.25, 55.83)	55.10	(53.26, 56.37)
	Beta	20.25	(19.43, 21.16)	20.13	(19.31, 20.86)	19.81	(18.93, 21.08)
	Alpha	8.43	(8.15, 8.76)	8.28	(8.06, 8.63)	8.45	(8.05, 8.82)
	Theta	3.67	(3.56, 3.81)	3.66	(3.53, 3.83)	3.74	(3.60, 3.90)
	Delta	1.61	(1.53, 1.66)	1.58	(1.53, 1.65)	1.61	(1.55, 1.69)

888

889 **Table S2:** Characteristic oscillation frequency summary statistics (medians and (25<sup>th</sup>, 75<sup>th</sup>) quartiles) for each  
890 group at each assessment age.

891

892

893



Node pair	Median Mutual Information (CAUG, FCG, NIG)	Regression Coefficient	Confidence Interval (CI)	Standard Error (SE)	p-value	Wald statistic
<b>Gamma Oscillation Connectivity</b>						
(P3, Pz)	0.096, 0.084, 0.073	-0.009	[-0.017, -5E-04]	0.004	0.037	4.44
(P4, O1)	0.024, 0.018, 0.014	-0.005	[-0.009, -3E-04]	0.002	0.038	4.40
(P4, O2)	0.059, 0.048, 0.040	-0.009	[-0.014, -0.003]	0.003	0.002	9.66
(Pz, O1)	0.051, 0.042, 0.036	-0.006	[-0.012, -0.002]	0.003	0.008	7.27
(Pz, O2)	0.053, 0.044, 0.037	-0.007	[-0.012, -0.002]	0.003	0.007	7.58
<b>Network</b>	0.054, 0.048, 0.041	-0.007	[-0.011, -0.003]	0.001	0.002	9.76
<b>Beta Oscillation Connectivity</b>						
(F3, F4)	0.028, 0.034, 0.047	0.005	[2.00E-04, 0.009]	0.002	0.042	4.25
(F3, T7)	0.016, 0.021, 0.031	0.005	[0.002, 0.009]	0.002	0.005	8.32
(F4, T7)	0.005, 0.009, 0.013	0.003	[0.001, 0.005]	0.001	0.002	9.83
(Fz, T7)	0.006, 0.010, 0.015	0.003	[0.001, 0.005]	9.20E-004	0.002	10.02
(C4, T7)	0.003, 0.005, 0.010	0.001	[1.00E-04, 0.003]	6.30E-004	0.030	4.82
(P3, Pz)	0.115, 0.096, 0.080	-0.008	[-0.014, -0.002]	0.003	0.016	5.98
(P3, T7)	0.018, 0.027, 0.035	0.004	[4.00E-04, 0.007]	0.002	0.030	4.86
(T7, T8)	0.008, 0.012, 0.019	0.004	[0.001, 0.007]	0.001	0.004	8.60
(T7, O1)	0.010, 0.017, 0.029	0.005	[0.001, 0.009]	0.002	0.008	7.23

(T7, O2)	0.008, 0.012, 0.022	0.004	[5.00E-04, 0.007]	0.002	0.023	5.36
<b>Network</b>	0.012, 0.016, 0.021	0.003	[5.00E-04, 0.006]	0.001	0.021	5.44
<b>Alpha Oscillation Connectivity</b>						
(F3, T7)	0.038, 0.047, 0.059	0.005	[3.00E-04, 0.009]	0.002	0.036	4.50
(F4, T7)	0.022, 0.028, 0.036	0.004	[3.00E-04, 0.007]	0.002	0.031	4.78
(Fz, T7)	0.021, 0.028, 0.035	0.004	[4.00E-04, 0.007]	0.002	0.029	4.89
(P3, Pz)	0.087, 0.073, 0.063	-0.007	[-0.011, -0.002]	0.002	0.009	6.99
(P4, Pz)	0.076, 0.067, 0.057	-0.005	[-0.010, -3.0E-04]	0.002	0.036	4.52
(P4, O2)	0.070, 0.062, 0.053	-0.005	[-0.009, -0.001]	0.002	0.012	6.56
(T7, O1)	0.026, 0.040, 0.051	0.005	[9.00E-04, 0.009]	0.002	0.018	5.76
(T7, O2)	0.021, 0.027, 0.037	0.005	[0.001, 0.009]	0.002	0.013	6.37
<b>Network</b>	0.022, 0.029, 0.038	0.004	[7.00E-04, 0.007]	0.001	0.017	5.9
<b>Theta Oscillation Connectivity</b>						
(Fz, Pz)	0.011, 0.010, 0.008	-0.001	[-0.0025, -2.0E-04]	5.70E-04	0.024	5.21
(Fz, T7)	0.019, 0.022, 0.027	0.002	[2.0E-04, 0.005]	0.001	0.031	4.80
(C3, P3)	0.047, 0.041, 0.035	-0.004	[-0.008, -3.0E-04]	0.002	0.032	4.71
(C4, P4)	0.046, 0.040, 0.035	-0.003	[-0.006, -2.0E-04]	0.001	0.036	4.53
(P3, P4)	0.059, 0.053, 0.047	-0.003	[-0.006, -3.0E-04]	0.001	0.030	4.80
(P3, Pz)	0.088, 0.081, 0.073	-0.005	[-0.009, -4.0E-04]	0.002	0.032	4.73
(P4, O1)	0.051, 0.043, 0.037	-0.004	[-0.007, -7.0E-04]	0.002	0.016	5.94

(P4, O2)	0.073, 0.063, 0.056	-0.007	[-0.011, -0.002]	0.002	0.003	9.28
(T7, T8)	0.035, 0.041, 0.050	0.004	[4.0E-04, 0.008]	0.002	0.027	4.98
(O1, O2)	0.118, 0.104, 0.097	-0.006	[-0.012, -6.0E-04]	0.003	0.031	4.78
<b>Network</b>	0.048, 0.043, 0.040	-0.002	[0.013, -7.0E-04]	9.0E-04	0.043	4.20

896

897

898

899

900

901

902

903

904

905

906

907

908

909

910

911

912

913

914

**Table S3:** Summary of statistics for linear regression models for pairwise connectivities at 96 months as a function of group with an adjustment for birth weight or head circumference at that age. Only the statistics for pairs of nodes with statistically distinct connectivity (edge) among 3 groups are shown, as well as averaged connectivity over the subnetwork defined by these nodes/edge pairs. Median MI values for each group are provided in column 2.

Node	Median Node Centrality (CAUG, FCG, NIG)	Regression Coefficient	Confidence Interval (CI)	Standard Error (SE)	p-value	Wald statistic
<b>42 MONTHS</b>						
Gamma Oscillation Node Connectedness						
T7	0.50, 0.42, 0.17	-0.117	[-0.187, -0.047]	0.035	0.001	10.89
Beta Oscillation Node Connectedness						
Fz	0.50, 0.42, 0.33	-0.086	[-0.153, -0.019]	0.034	0.012	6.41
T7	0.67, 0.50, 0.33	-0.115	[-0.192, -0.039]	0.039	0.003	9.00
T8	0.67, 0.42, 0.17	-0.078	[-0.152, -0.004]	0.038	0.040	4.28
Alpha Oscillation Node Connectedness						
Pz	0.67, 0.50, 0.42	-0.078	[-0.143, -0.014]	0.033	0.018	5.75
Theta Oscillation Node Connectedness						
Fz	0.50, 0.33, 0.25	-0.092	[-0.152, -0.033]	0.030	0.002	9.56
Pz	0.58, 0.50, 0.42	-0.101	[-0.165, -0.037]	0.032	0.002	9.77
<b>96 MONTHS</b>						
Gamma Oscillation Node Connectedness						
Pz	0.50, 0.42, 0.33	-0.080	[-0.149, -0.011]	0.035	0.024	5.23
Beta Oscillation Node Connectedness						
Pz	0.58, 0.5, 0.42	-0.094	[-0.156, -0.033]	0.031	0.003	9.22
T7	0.08, 0.17, 0.25	0.079	[0.016, 0.142]	0.032	0.015	6.09

Alpha Oscillation Node Connectedness						
C3	0.50, 0.33, 0.25	-0.089	[-0.162, -0.016]	0.037	0.017	5.87
C4	0.42, 0.33, 0.17	-0.082	[-0.152, -0.013]	0.035	0.021	5.48
P4	0.50, 0.42, 0.33	-0.068	[-0.134, -0.001]	0.034	0.047	4.00
Pz	0.58, 0.42, 0.33	-0.083	[-0.147, -0.020]	0.032	0.011	6.68
T7	0.17, 0.42, 0.50	0.070	[0.001, 0.140]	0.035	0.048	3.98
Theta Oscillation Node Connectedness						
Fz	0.42, 0.33, 0.25	-0.077	[-0.135, -0.018]	0.030	0.011	6.58
C3	0.50, 0.42, 0.33	-0.085	[-0.158, -0.012]	0.037	0.022	5.32
C4	0.42, 0.33, 0.25	-0.070	[-0.140, -0.001]	0.035	0.047	4.00
P4	0.50, 0.42, 0.33	-0.067	[-0.130, -0.005]	0.032	0.035	4.51
Pz	0.58, 0.50, 0.33	-0.094	[-0.160, -0.030]	0.033	0.005	8.28

915

916 **Table S4:** Summary of statistics for linear regression models node connectedness (centrality based on the total  
917 number of connections), for each oscillation network at 42 and 96 months. Only the statistics for the 'group'  
918 parameter are shown, for nodes that were statistically distinct in the 3 groups when adjusted for birth weight or  
919 head circumference. Median connectedness values for each group are provided in column 2.

920

921

922

923

924

925  
 926  
 927  
 928  
 929  
 930  
 931  
 932  
 933  
 934  
 935  
 936  
 937  
 938  
 939  
 940  
 941

Node	Median Node Centrality (CAUG, FCG, NIG)	Regression Coefficient	Confidence Interval (CI)	Standard Error (SE)	p-value	Wald statistic
Gamma Oscillation Node Strength						
Pz	0.1165, 0.1091, 0.1032	-0.004	[-0.008, -7E-04]	0.002	0.048	3.99
Beta Oscillation Node Strength						
F3	0.1019, 0.1037, 0.1056	0.002	[1E-04, 0.004]	0.001	0.034	4.63

F4	0.1005, 0.1024, 0.1047	0.002	[3E-04, 0.004]	0.001	0.019	5.69
Fz	0.1007, 0.1021, 0.1038	0.001	[1E-04, 0.003]	0.001	0.036	4.51
Pz	0.1122, 0.1106, 0.1084	-0.002	[-0.004, -1E-04]	0.001	0.048	3.99
T7	0.0943, 0.0974, 0.1011	0.003	[0.001, 0.005]	0.001	0.002	10.55
Alpha Oscillation Node Strength						
P4	0.1146, 0.1100, 0.1061	-0.002	[-0.003, -1E-04]	0.001	0.041	4.28
Pz	0.1125, 0.1084, 0.1050	-0.002	[-0.003, -9E-05]	0.001	0.050	3.84
T7	0.1095, 0.1123, 0.1146	0.003	[2E-04, 0.005]	0.001	0.038	4.40
Theta Oscillation Node Strength						
P4	0.1173, 0.1151, 0.1139	-0.002	[-0.003, -4E-04]	0.001	0.012	6.49
T7	0.1067, 0.1104, 0.1143	0.002	[1E-04, 0.004]	0.001	0.040	4.33

942

943

944

945

946

947

948

949

950

**Table S5:** Summary of statistics for linear regression models node strength (centrality based on the sum of node weights), for each gamma, beta, alpha and theta networks at 96 months. Only the statistics for nodes that were statistically distinct in the 3 groups when adjusted for birth weight or head circumference are shown. Median node strength values for each group are provided in column 2.

Node pair	Regression	Confidence	Standard Error	p-value	Wald statistic
-----------	------------	------------	----------------	---------	----------------

	Coefficient	Interval (CI)	(SE)		
<b>Gamma Oscillation Connectivity (Network Edge) Trajectory</b>					
(C3, P3)	-0.016	[-0.030, -0.002]	0.007	0.024	5.13
(P3, Pz)	-0.019	[-0.033, -0.005]	0.007	0.007	7.29
(P3, O2)	-0.012	[-0.023, -0.001]	0.006	0.029	4.80
(P4, O1)	-0.011	[-0.022, -0.001]	0.005	0.032	4.65
(P4, O2)	-0.014	[-0.025, -0.003]	0.006	0.014	6.10
(Pz, O2)	-0.011	[-0.022, -0.001]	0.005	0.031	4.69
<b>Beta Oscillation Connectivity (Network Edge) Trajectory</b>					
(P3, Pz)	-0.005	[-0.011, -1E-04]	0.003	0.050	3.80
<b>Alpha Oscillation Connectivity (Network Edge) Trajectory</b>					
(P3, Pz)	-0.006	[-0.011, -0.001]	0.003	0.049	3.90
(P4, O2)	-0.006	[-0.011, -0.001]	0.003	0.05	3.89
<b>Theta Oscillation Connectivity (Network Edge) Trajectory</b>					
(P3, Pz)	-0.008	[-0.012, -0.002]	0.002	0.015	6.03
(P4, O2)	-0.007	[-0.012, -0.002]	0.002	0.010	6.82

951

952 **Table S6a:** Summary of linear mixed effects regression models statistics for pairwise connectivity trajectories  
953 from 42 to 96 months, as a function of time and group, adjusted for birth weight and/or head circumference.  
954 Only the statistics for the 'group' parameter are shown, for pairs of nodes for which their connectivity (edge)  
955 was statistically distinct in the 3 groups.



956  
 957  
 958  
 959  
 960  
 961  
 962

Node	Regression Coefficient	Confidence Interval (CI)	Standard Error (SE)	p-value	Wald statistic
Alpha Oscillation Node Connectedness Trajectory					
P4	-0.053	[-0.088, -0.017]	0.018	0.004	8.60
Pz	-0.035	[-0.066, -0.003]	0.016	0.030	4.77
Theta Oscillation Node Connectedness Trajectory					
P4	-0.045	[-0.087, -0.003]	0.021	0.036	4.44
Pz	-0.040	[-0.073, -0.007]	0.017	0.018	5.71

963

964 **Table S6b:** Summary of linear mixed effects regression models statistics for the trajectories of node  
 965 connectedness from 42 to 96 months, as a function of time and group, adjusted for birth weight and/or head  
 966 circumference. Only the statistics for the 'group' parameter are shown, for pairs of nodes that were statistically  
 967 distinct in the 3 groups.

968

969

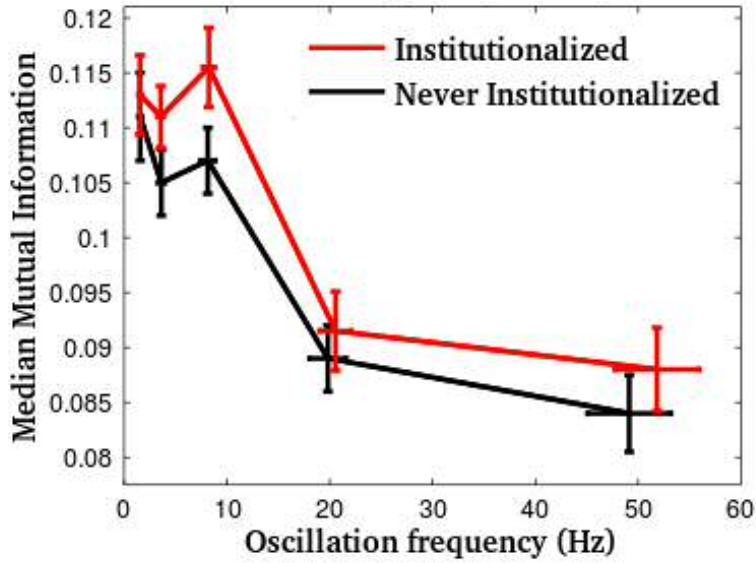
970

971

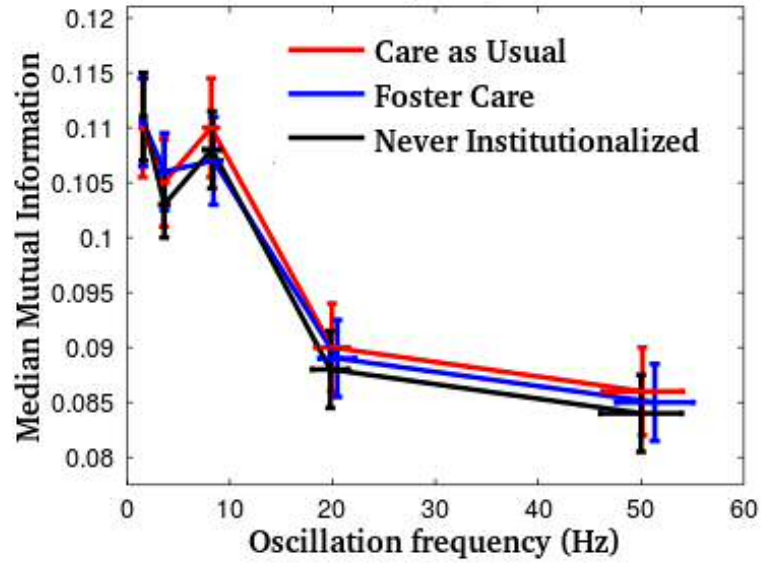
972

973

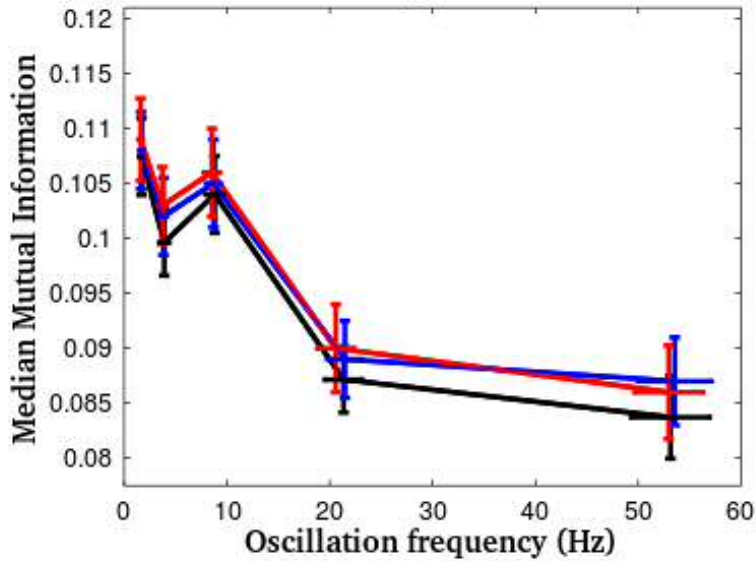
First time point (<30 mo)



Second time point (30-33 mo)



Third time point (42 mo)



Fourth time point (96 mo)

